Materials Design Rules for Multi-Valent Ion Mobility in Intercalation Structures –Supporting Information–

Ziqin Rong,[1] Rahul Malik,[1] Pieremanuele Canepa,[1] Gopalakrishnan Sai Gautam,[1] Miao Liu,[2] Anubhav Jain,[2] Kristin Persson,[2] and Gerbrand Ceder[1]

[1]*The Department of Materials Science and Engineering, Massachusetts Institute of Technology, Cambridge MA 02139, USA.* [2]*Environmental Energy Technologies Division, Lawrence Berkeley National Laboratory, CA 94720, USA*

1.1 Computational Details

To model the ionic diffusion in the selected host structures, we use nudged elastic band (NEB)[11] simulations coupled with density functional theory (DFT), specifically the Perdew–Burke–Ernzerhof[2] Generalized-Gradient Approximation (GGA), as implemented in VASP. We elected to use GGA over GGA+*U* for the reasons previously indicated by Liu *et al.*[3] for first-principles calculations of MV ion migration in oxide spinels, namely the pronounced metastability of electronic states along the ion migration path with +*U* which results in poor computational convergence, and also the lack of conclusive evidence that +*U* performs better in determining the cation migration barriers.

The total energy was sampled using a Monkhorst-Pack mesh with *k*-point density of 1000/(number of atoms per unit cell). Projector augmented-wave theory[4] combined with a well-converged plane-wave cutoff of 520 eV were used to describe the wave functions. The convergence threshold of the total energy was set to 1×10^{-5} eV, and a tolerance of 0.1 eV/Å for the forces was used to converge the minimum energy path (MEP) in the NEB procedure. The initial MEPs were prepared by linear interpolation

between the end-points using 8 images (or 9 for V_2O_5). In order to avoid spurious interactions between images, supercells of appropriate sizes were used ensuring a minimum inter-image distance of 8 Å.

With the computational parameters described above, we performed the NEB calculations on several host-structure while changing the diffusing species of interest. The host-structures considered are $FePO_4$ (olivine), Mn_2O_4 (spinel), NiO_2 (layered), V_2O_5 (pseudo-layered), while the moving species chosen were Li^+, Ca^{2+}, Mg^{2+}, Zn^{2+}, and Al^{3+}. The analysis of the MEP not only gives the topology of the diffusing species, but also provides information about the host-structure perturbation. The maximum energy value of the MEP represents the migration barrier that is reported in this work.

For the calculation of voltages and capacities (see Sec. 1.5) DFT+*U* (PBE+*U*) was used to correct for the self-interaction error introduced by the highly localized *d* orbitals of the redox species V, Mn, Fe, and Ni. The *U* values were set to 3.25 eV for V, 3.1 eV for Mn, 5.3 eV for Fe and 6.45 eV for Ni, respectively.

1.2 Al^{3+} Calculations in Olivine $FePO_4$ and Layered NiO_2

NEB calculations for Al^{3+} are particularly challenging to converge in olivine $FePO_4$ and layered NiO_2 due to the highly localized charge on the Al^{3+} species and the strong thermodynamic instability of Al^{3+} in these two host structures resulting in especially large forces on the host lattice (which consequently make convergence difficult). For this reason we presented only the MEP of Al^{3+} in Mn_2O_4 and V_2O_5. In lieu of NEB

results for olivine $FePO_4$ and layered NiO_2, we have calculated the site energy difference E_t–E_s between Al^{3+} residing in the initial octahedral site and the intermediate tetrahedral site along the diffusion path. For both of these cases, we find Al^{3+} occupation of the intermediate tetrahedral site is indeed lower in energy (by ~ 136 meV for olivine $FePO_4$, and ~ 226 meV for layered NiO_2), verifying the thermodynamic instability of Al^{3+} in these structures.

1.3 Estimation criteria for E_m cutoff

An upper bound for the MV migration barrier E_m can be established from reasonable battery performance criteria: a 2 hour (dis)charge time t (or C/2 rate) for a 1 μm active particle size suggests a minimum diffusivity $D \sim 10^{-12}$ cm^2s^{-1} given the diffusion length scales as $\sqrt{Dt}$. Using a random walk for diffusion sets a maximum $E_m \sim 525$ meV that can be tolerated, assuming $D \approx \nu \cdot a^2 \cdot exp(-E_m/kT)$ with atomic jump frequency $\nu \approx 10^{12}$ s^{-1} and atomic jump distance $a \approx 3$ Å, the length of a typical lattice parameter. For every order of magnitude particle size reduction this tolerance increases by ~ 125 meV. Hence, 100 nm crystallites could be charged and discharged in 2 hours when barriers are less than ~ 650 meV. Note that reasonable ion diffusion is a required condition for cathode materials, but it is by no means sufficient as other phenomena, either in the cathode (e.g. phase transformations, conductivity) or in the cell, can be rate limiting. Nonetheless, solid-state diffusion is widely seen as the most challenging design problem for MV-cathode materials.

1.4 NiO_2 Oxygen Dumbbell Hop

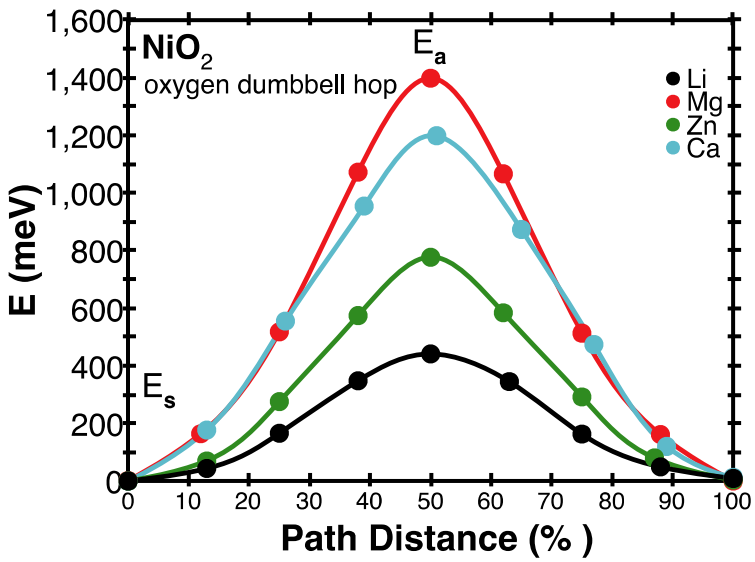

Figure S1: Energies for MV ion migration (Li^+, Mg^{2+}, Zn^{2+}, Ca^{2+}) for the oxygen dumbbell hop in layered NiO_2, which correspond to MV ion motion through a O–O bond (labeled as E_a), are higher for each ion than migration through the intermediate tetrahedral site shown in **Figure 1c**.

1.5 Comparison to First-Principles data for Orthorhombic V_2O_5 in the literature

Carrasco *et al.*[5] and Zhou *et al.*[6] both have investigated Mg^{2+} intercalation in orthorhombic V_2O_5 polymorphs using first-principles NEB calculations, but with some deviation from our outlined computational procedure. Carrasco *et al.* investigated Li^+, Mg^{2+}, and Ca^{2+} migration in the de-intercalated α–V_2O_5 polymorph (note in this work we have focused on the δ polymorph), incorporating both $+U$ and van der Waal's interactions in their calculations, and obtained migration energies of ~ 310, ~ 980 and ~1800 meV for Li^+, Mg^{2+}, and Ca^{2+}, respectively. Using the parameters outlined in the **Computational Details** section, we performed calculations in the same structure and obtained very good agreement for Mg^{2+} (975 meV) and Ca^{2+} (1700 meV), but a lower value for Li^+ (150 meV) as also noted in Carrasco's work.

Zhou *et al.* investigated Mg^{2+} diffusion in both the deintercalated α and δ polymorphs, and obtain a much higher value for α, >1200 meV compared to ~ 975 – 980 meV as indicated by our calculations and calculations performed by Carrasco. For the δ polymorph, the shape of the migration energy has the same "valley" shape as seen in **Fig 3** in this work, but both the migration barrier and intermediate site energy determined by Zhou *et al.* are much higher, >1800 meV compared to 680 meV for the migration barrier, and 800 meV compared to less than 200 meV for the intermediate site energy. We speculate that the differences originate from two discrepancies in computational procedure. First, for some calculations Zhou *et al.* allow only the Mg ions and nearby oxygen ions to move which impedes convergence to the MEP, and second, we found that using an odd number of images (9 as opposed to 8) has a significant effect on improving convergence to the MEP by allowing the middle image to occupy the low-energy intermediate site, which is observed for all MV cations considered in both the charged and discharged limits as observed in **Fig 3**.

1.6 Voltages and Capacity of multivalent cathodes

Table S1 shows the voltages and specific capacities of the materials discussed in the paper calculated from first-principle calculations (see Sec. 1.1).

Table S1: Voltages and Specific Capacities of M_xNiO_2, M_xFePO_4, $M_xMn_2O_4$, δ-$M_xV_2O_5$ (M = Mg, Ca, Zn). The subscripts under *M* (Zn, Mg, Ca) specify the amount of intercalation considered for these values.

Formula	Voltage (V)	Capacity (mAh/g)
	Mn_2O_4	
$Mg_{0\sim0.5}Mn_2O_4$	2.86	270
$Ca_{0\sim0.5}Mn_2O_4$	3.15	251
$Zn_{0\sim0.5}Mn_2O_4$	1.60	224
	NiO_2	
$Mg_{0\sim0.25}NiO_2$	3.50	138
$Ca_{0\sim0.25}NiO_2$	4.02	133

$\mathbf{Zn_{0\sim0.25}NiO_2}$	1.98	125
	$FePO_4$	
$\mathbf{Mg_{0\sim0.5}FePO_4}$	3.24	164
$\mathbf{Ca_{0\sim0.5}FePO_4}$	4.10	157
$\mathbf{Zn_{0\sim0.5}FePO_4}$	1.68	146
	δ-V_2O_5	
$\mathbf{Mg_{0\sim1}V_2O_5}$	2.56	260
$\mathbf{Ca_{0\sim1}V_2O_5}$	3.04	242
$\mathbf{Zn_{0\sim1}V_2O_5}$	1.11	217

The average voltage data calculated is given by:

$$V = -\frac{G[M_{x_2}Host] - G[M_{x_1}Host] - (x_2 - x_1)G[M]}{x_2 - x_1} \quad (1)$$

where G the Gibbs free energy of the compound is approximated by the DFT total energy at 0 K, and x_1 and x_2 are the fractions of MV cation intercalated respectively. The specific capacity of the intercalation compound is given by:

$$Capacity = \frac{2V(x_2 - x_1)}{m[M_{x_2}Host] + m[M_{x_1}Host]} \quad (2)$$

where V is the average voltage (from Eq. 1) and m is the mass of the compound.

References

1. D. Sheppard, R. Terrell, and G. Henkelman, Optimization methods for finding minimum energy paths. *J. Chem. Phys.*, 2008, **128**, 134106.
2. J. P. Perdew, K. Burke, and M. Ernzerhof, Generalized gradient approximation made simple, *Phys. Rev. Lett.*, 1996, **77**, 3865–3868.
3. M. Liu, Z. Rong, R. Malik, P. Canepa, A. Jain, G. Ceder, and K. A. Persson, Spinel compounds as multivalent battery cathodes: a systematic evaluation based on ab initio calculations, *Energy Environ. Sci.*, 2014, **8**, 964–974.
4. G. Kresse and D. Joubert, From ultrasoft pseudopotentials to the projector augmented-wave method, *Phys. Rev. B*, 1999, **59**, 1758–1775.
5. J. Carrasco, Role of van der Waals Forces in Thermodynamics and Kinetics of Layered Transition Metal Oxide Electrodes: Alkali and Alkaline-Earth Ion Insertion into V_2O_5, *J. Phys. Chem. C*, 2014, **118**, 19599–19607.
6. B. Zhou, H. Shi, R. Cao, X. Zhang, and Z. Jiang, Theoretical study on the initial stage of a magnesium battery based on a V_2O_5 cathode, *Phys. Chem. Chem. Phys.*,

2014, **16**, 18578.